



# Study of Heat Transfer in the Walls of the Body Superstructure of a Vehicle for Transporting Frozen Meat Carcasses

Horia Beles<sup>(✉)</sup>, Iulian Stanasel, Dan Craciun, Florin Bogdan Scurt,  
and Bogdan Adrian Tolea

University of Oradea, Universitatii Street, No. 1, Oradea, Romania

**Abstract.** The scientific paper presents a study on heat transfer in the sandwich walls of the body superstructure of a vehicle for transporting frozen meat carcasses. The transport of perishable products (dairy products, meat, ice cream, vegetables, medicines, etc.) requires particular attention, both to avoid product spoilage and economic losses, but above all to avoid damage to consumer health. This paper presents a thermal analysis of an area of the side wall of a refrigerated structure designed to transport meat carcasses on hooks. The simulation of heat transfer through the layers of such a refrigeration panel was performed using ANSYS software. The thermally analysed wall area includes the stiffening element, as it has an important influence on heat transfer.

**Keywords:** Transfer · Body Superstructure · Vehicle for Transporting Frozen Meat Carcasses

## 1 Introduction

Perishable products such as meat, fish, vegetables, fruit and dairy products must be kept chilled or frozen throughout the supply chain [1]. The supply chain consists of several stages, some of which are: harvesting or processing of the raw material, pre-freezing, storage before distribution, transport to distribution centres and shops, consumer pick-up and consumer storage [1].

It is well known that refrigeration or freezing, food quality and food waste are closely linked [1, 2].

According to [1], the United Nations estimates that annually about 1/3 of all food produced for human consumption is wasted, while other sources indicate that food wastage is as high as 40% of production [1].

Thus, in 1970, the United Nations drew up an Agreement on the International Transport of Perishable Foodstuffs (ATP). This agreement contains all the regulations for almost all types of refrigerated vehicles used for the transportation of perishable goods [3].

According to the ATP document, several standards are regulated for the overall heat transfer coefficient (K), which can be determined analytically or experimentally.

In the same agreement [3], but also in its updates, there is information that makes it possible to classify isothermal transport vehicles on the basis of the overall heat transfer coefficient but also on the basis of the temperature that the cooling and ventilation unit can produce. Thus, the following two types can be found:

- a. normal isothermal transport means IN, is defined by an overall heat transfer coefficient,  $K = 0,7 \text{ W/m}^2 \cdot \text{K}$ .
- b. reinforced isothermal transport medium IR, characterized by an overall heat transfer coefficient,  $K = 0,4 \text{ W/m}^2 \cdot \text{K}$ .

In the case of vehicles intended for the transport of perishable goods, namely frozen meat on hooks, they must have an overall heat transfer coefficient less than or equal to  $0,4 \text{ W/m}^2 \cdot \text{K}$  for a temperature range of 0 to  $-25 \text{ }^\circ\text{C}$  or colder [1, 3].

According to [4], in 2010, there were about 4 million refrigerated road vehicles worldwide, and the number is expected to increase by 2,5% per year by 2030. However, in order to limit this increase in the number of refrigerated vehicles, and especially the pollution they generate, it would be necessary to improve the structure or materials of the insulating walls, which will lead to a reduction in energy consumption for achieving low temperatures [4].

In addition, the materials from which these insulating panels are made are subject to quite harsh conditions (repeated cooling and heating), which accelerates their ageing process and thus reduces their thermal performance. Due to the infiltration of water vapour and working fluids, insulation materials significantly reduce their performance [4–8].

A fairly widely used material for refrigerated vehicles, according to [7], is polyurethane foam (PU), with good mechanical strength, low cost and low water retention [4].

The outer areas of the panel are often made of polyester (PE) or Acrylonitrile Butadiene Styrene (ABS), based composite material. This composite material consists of a combination of resin (polyester PE or ABS) and reinforced fiberglass (FG), to achieve quite good mechanical and chemical resistance. Polyester is known to be used for its ability to maintain its mechanical properties even at low temperatures [4].

The aim of this work is to analyse the heat transfer for a refrigerated panel area with 3 types of metal profiles that could make up the strength structure of the cold box.

Such an area has been chosen because it has been found over time that the portion located in front of the metal stiffening element, yields much more easily the temperature.

*Characteristics of the panel.* Typically, vehicles with a superstructure used for the transport of frozen food are constructed of insulating sandwich panels, which may be made of different types of materials (fiberglass, foam, aluminium plates, etc.). These panels must also include elements for the strength structure, which are often made of steel in various configurations. Table 1 shows the sizes and units of measurement used in this paper, and Table 2 shows the coefficient of thermal conductivity for all three basic materials used in the panel structure.

The piece of panel analysed has the following dimensions:  $2000 \times 500 \times 65 \text{ mm}$ .

**Table 1.** Sizes and units of measurement used.

Size	Name of size	Units
Q	quantity of heat	W
A	heat transfer surface	m <sup>2</sup>
q	specific heat load	W/m <sup>2</sup>
r	thermal resistance of the wall	m · deg/W
t <sub>1</sub> ,t <sub>2</sub>	surface temperatures	K
Δt <sub>m</sub>	average temperature difference	K
k	total heat transfer coefficient	W/m <sup>2</sup> · deg
λ	coefficient of thermal conductivity	W/m · K

**Table 2.** Thermal coefficient

Material	Thermal coefficient values	Units measurement
steel	60,5	W/m · K
foam	0,28	W/m · K
fiber glass	0,04	W/m · K

The fiberglass on the inside of the cold box has a higher mechanical strength than the outside, because on the inside during the movement of the vehicle the meat hanging on the hooks can hit the walls of the cold box.

## 2 Heat Transfer Analysis

Heat transfer analysis is used to determine the effects that conduction, convection and radiation can have on a structure. Heat transfer can occur during a steady state or over time with transient analysis. Material properties, heat transfer coefficients and heat flux, can be temperature dependent. Flow conditions can be set for forced convection, and view factor calculations performed for radiation analysis, as well as many other factors, which help determine the behavior of a system when thermal conditions are involved, will be presented below.

The equation of steady-state conductivity heat transfer through a flat, single-layer wall can be determined from Fig. 1.

Unit heat flow/flux:

$$q = \frac{Q}{A} = \frac{t_1 - t_2}{r} = \frac{\lambda}{\delta}(t_1 - t_2) \quad (1)$$

Thermal resistance of the wall:

$$r = \frac{\delta}{\lambda} = \frac{1}{\alpha} \quad (2)$$

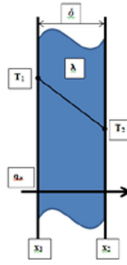


**Fig. 1.** Temperature variation through a homogeneous flat wall

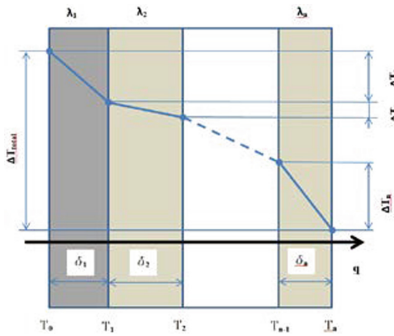


**Fig. 2.** Conductive heat transfer through flat composite walls

Total heat flow/flux:

$$q = \frac{Q}{A} = K \cdot A \cdot \Delta t_m \tag{3}$$

To determine the equation for steady-state heat transfer through a wall made of several parallel layers, it is assumed that in the steady state the heat fluxes through each layer are equal to each other.

Figure 2 shows the temperature variation through the layers.

$$q = \frac{\lambda_1}{\delta_1} \Delta t_1 = \frac{\lambda_2}{\delta_2} \Delta t_2 = \dots = \frac{\lambda_n}{\delta_n} \Delta t_n \tag{4}$$

$$Q = \frac{(t_1 - t_2) \cdot A}{\frac{\delta_1}{\lambda_1} + \frac{\delta_2}{\lambda_2} + \dots + \frac{\delta_n}{\lambda_n}} \tag{5}$$

The total heat transfer coefficient (K) is determined with the following relation:

$$K = \frac{1}{\frac{1}{\alpha} + \sum \frac{\delta}{\lambda}} \tag{6}$$

Heat is transferred from warm air (turbulent flow, which is determined from the Reynolds criterion value). The partial heat transfer coefficient is determined with the relation:

$$Nu = \frac{\alpha \cdot l}{\lambda} \quad (7)$$

where: Nu - represents the Nusselt criterion

For the case of air flow on flat surfaces, the Nusselt criterion is described by the relation:

$$Nu = 0.032 \cdot Re^{0.8} \quad (8)$$

The (dimensionless) Reynolds number calculation for the flat plate is performed with the relation:

$$Re = \frac{\rho \cdot v \cdot L}{\mu} \quad (9)$$

The meaning of the terms in the above relationship is as follows:

$\rho$  – fluid density [kg/m<sup>3</sup>]

$v$  – fluid flow velocity [m/s]

$L$  – plate length characteristic [m]

$\mu$  – fluid viscosity [N · s/m<sup>2</sup>]

For air, the following values were taken into account:

$\rho = 1,164$  [kg/m<sup>3</sup>]

$v = 25$  [m/s]

$L$  – is determined with relation 10.

$$L = \frac{4S}{P} \quad (10)$$

$S$  – surface of the plate, [m<sup>2</sup>]

$P$  – perimeter, [m]

After performing the calculations, it will obtain:

$L = 0,8$  m

$\mu = 18,6 \cdot 10^{-6}$  [N · s/m<sup>2</sup>]

The calculation show that:

$Re = 1,252 \cdot 10^6$  (turbulent flow is outside the chamber)

$Nu = 2,416 \cdot 106$ .

Knowing the thermal conductivity coefficient for air  $\lambda_{air} = 0,025$  [W/m · K], it follows:

$$\alpha_{air} = \lambda_1 \frac{Nu}{L} = 72,48 \text{ [W/m} \cdot \text{K]} \quad (11)$$

For the fiberglass wall, the thermal conductivity coefficient  $\lambda_{fiberglass} = 0,04$  [W/m · K], the wall thickness  $\delta_{fiberglass} = 0,005$  [m] are known and can be obtained:

$$\alpha_{fiber} = 8 \text{ [W/m} \cdot \text{K]}$$

The calculations were based on [9] and [10].

### 3 Computational Simulation

#### 3.1 Initial Condition

After 3D modelling of the three types of cold room wall panels, thermal behaviour analysis was performed for the steady state using.

The initial conditions as well as the material properties were set in the software settings. The data entered for convective heat transfer were as shown in Table 2. When performing the heat transfer analysis, the adhesive used in the production of refrigerated panels was not taken into account, as it has no significant influence on the thermal properties.

The geometry of the panel used for the simulation is a simple parallelepiped with a transfer area of 1 m<sup>2</sup>. The number of finite elements is between 14.400 and 19.600, since it varies with the modification of the metallic stiffening element.

In order to carry out the heat transfer simulation of the three types of panels, an estimated temperature between -18 and 0 °C was applied to the inner wall of the panel and an average temperature between 25 and 30 °C was applied to the outer wall of the panel in order to reproduce as well as possible real working and test situations, according to [3]. In most types of insulating panels, the metal stiffening elements are in direct contact with the inner fiberglass wall.

#### 3.2 Thermal Analysis of Insulating Panel with Rectangular Pipe Stiffening Elements

In this case, the analysis was carried out on the area of the panel that has a rectangular pipe as a stiffening element. The presence of air inside the rectangular pipe was also taken into account, air being a good thermal insulator. Figure 3 shows the structure of the insulating panel with rectangular pipe-type stiffening element.

The simulation was carried out in the following way: a heat source was applied to the outer wall of the panel and then the temperature distribution through its materials was observed, showing a more intense heat transfer in the area of the metallic stiffening element. Figure 4 shows the temperature evolution across panel thickness and panel width respectively.

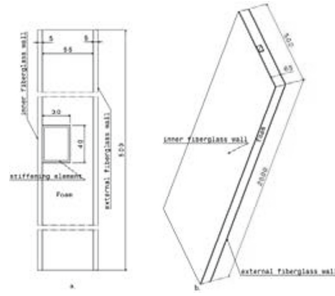


**Fig. 3.** Insulating panel structure with rectangular pipe-type stiffening element: a-top view; b-isometric view.

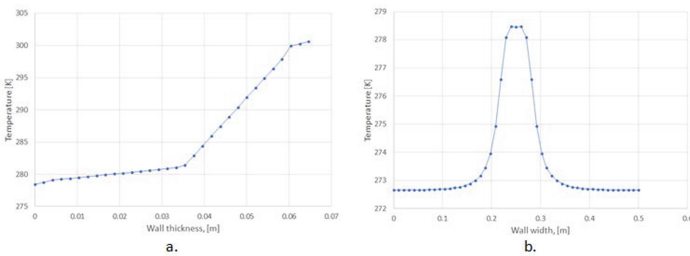


**Fig. 4.** Temperature evolution: a-over panel thickness; b-over and panel width.

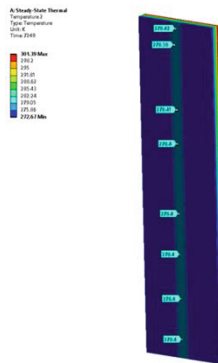
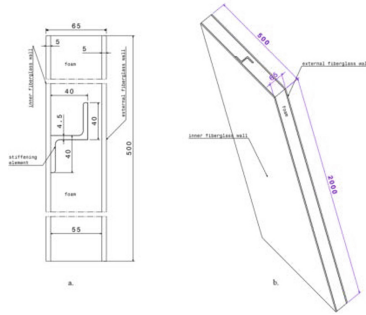


**Fig. 5.** Temperature evolution through panel layers.

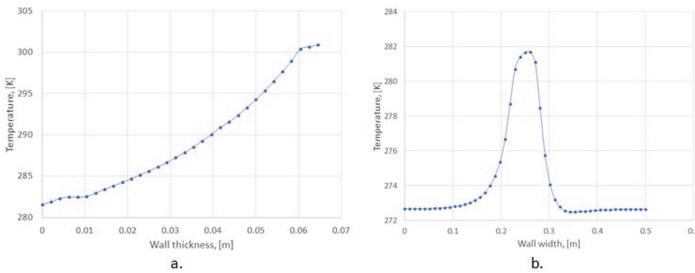
Figure 4.(a) shows the influence of air in the stiffening element cavity, through a slight temperature variation when the heat flux transmission reaches that area.

Figure 5 shows the temperature evolution through the panel layers.

In Fig. 5 it can be seen that the highest temperature on the inner layer of the panel is in the area of the stiffening element. Temperature find of 278,4 K, while on the rest of the surface a temperature of 272,67 K is found.



**Fig. 6.** Insulating panel structure with Z-type stiffening element: a-top view; b-isometric view.



**Fig. 7.** Temperature evolution: a-over panel thickness; b-over panel width.

### 3.3 Thermal Analysis of Insulating Panel with Z-profile Stiffening Element

In this simulation, the only difference to the panel structure is the replacement of the rectangular metal profile with a Z profile, DIN1027 (Z40x40x4.5). Figure 6 shows the structure of the insulating panel with Z-type stiffening element.

Figure 7 shows the temperature evolution across panel thickness and panel width respectively.

Figure 8 shows the same phenomenon as in the previous case. The highest temperature of the inner wall is in the area of the stiffening element, this temperature value is 281,62 K, with 3,21 K higher than in the previous case.

Figure 8 shows the temperature evolution through the panel layers.

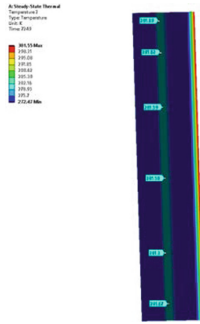
### 3.4 Thermal Analysis of Insulating Panel with T-profile Stiffening Element

For this analysis, a T40 DIN10055 profile was used as the stiffening element of the panel. Figure 9 shows the structure of the insulating panel with T-type stiffening element.

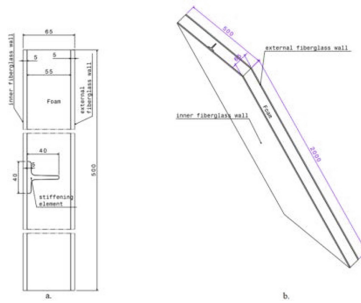
Figure 10 shows the temperature evolution across panel thickness and panel width respectively.

Figure 11 shows the temperature evolution through the panel layers.





**Fig. 8.** Temperature evolution through panel layers.



**Fig. 9.** Insulating panel structure with T-type stiffening element: a-top view; b-isometric view.

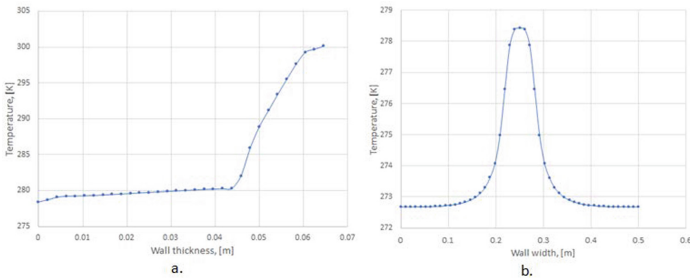


**Fig. 10.** Temperature evolution: a-over panel thickness; b-over panel width.

In the case of this panel with a T-type stiffening element, it can be seen that the temperature value on the inner wall in the area of the stiffening element is very close to that of the first case analysed, but still slightly lower.

But it can be seen that between the rectangular profile and the T-type profile there is a very small thermal difference of about 0,03K.

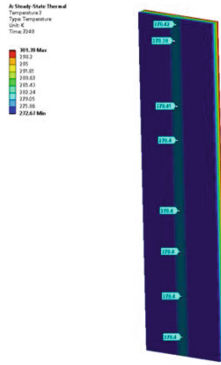


Fig. 11. Temperature evolution through panel layers.



Fig. 12. Comparison of temperature evolution in the stiffening element area.

### 4 Conclusion

This paper presented an analysis of heat transfer through insulating panels of refrigerated vehicles, carried out using ANSYS simulation software. The area that has been carefully examined is the area around the stiffening element because, as observed from the simulations, this is where the most intense thermal evolution occurs. Figure 12 shows the comparison of the temperature evolution in the stiffening element area for those three types of panels.

A comparison of the temperature evolution of the three types of panels shows that the panel using a T-type stiffening profile has the lowest heat transfer. The value of the temperature exchanged with the external environment, being very close to the panel with stiffening element made of rectangular pipe. The temperature difference in the simulations of the two panels mentioned above is about 0,03 K. Thus, it can be said that the use of a Z-type profile is the most thermally disadvantageous of the three types of profiles analysed with finite elements.

Another important point to note is that this paper did not analyse the variation of panel strength as a function of stiffening element profile. This is the subject of future research.

**Acknowledgments.** The research has been funded by the University of Oradea, within the Grants Competition “Scientific Research of Excellence Related to Priority Areas with Capitalization through Technology Transfer: INO - TRANSFER - UO”, Project No. 313/21.12.2021.

## References

1. Samuel Mercier, Sebastien Villeneuve, Martin Mondor, and Ismail Uysal: Time Temperature Management Along the Food Cold Chain A Review of Recent Developments. *Comprehensive Reviews in Food Science and Food Safety* Vol. 00, (2017).
2. Paúl B. Torres Jara, Juan J. Aguirre Rivera, Carlos E. Buenaño Merino, Efrén Vázquez Silva\*, Gabriela Abad Farfán.: Thermal behavior of a refrigerated vehicle: Process simulation, *International Journal of Refrigeration*, (2018).
3. UNECE Transport Division, United Nations. Agreement on the international carriage of perishable foodstuffs and on the special equipment to be used for such carriage (ATP), Geneva, Switzerland, (1970).
4. Patrick Glouannec, Benoit Michel, Guillaume Delamarre, Yves Grohens.: Experimental and numerical study of heat transfer across insulation wall of a refrigerated integral panel van. *Applied Thermal Engineering*, Elsevier, 196-204 (2014).
5. So, J.-H., Joe, S.-Y., Hwang, S.-H., Jun, S., Lee, S.-H.: Analysis of the Temperature Distribution in a Refrigerated Truck Body Depending on the Box Loading Patterns. *Foods* (2021).
6. G. Panozzo, G. Minotto, A. Barizza.: Transport et distribution de produits alimentaires: situation actuelle et tendances futures, *International Journal of Refrigeration*, Volume 22, Issue 8, (1999).
7. S.A. Tassou, G. De-Lille, y.T. Ge. Food transport refrigeration - approaches to reduce energy consumption and environmental impacts of road transport. *Applied Thermal Engineering*, Elsevier, pp.1467. (2009).
8. S.K. Chatzidakis, K.S. Chatzidakis.: Refrigerated transport and environment, *International Journal of Energy Research*. (2004).
9. K.F. Pavlov, P.G. Romankov, and A.A. Noskov.: *Procese și aparate în ingineria chimică - exerciții și probleme*, Editura Tehnică, București, (1981).
10. L. Gavrilă, *Fenomene de transfer*, Editura Alma Mater, Bacau, (2000).

**Open Access** This chapter is licensed under the terms of the Creative Commons Attribution-NonCommercial 4.0 International License (<http://creativecommons.org/licenses/by-nc/4.0/>), which permits any noncommercial use, sharing, adaptation, distribution and reproduction in any medium or format, as long as you give appropriate credit to the original author(s) and the source, provide a link to the Creative Commons license and indicate if changes were made.

The images or other third party material in this chapter are included in the chapter’s Creative Commons license, unless indicated otherwise in a credit line to the material. If material is not included in the chapter’s Creative Commons license and your intended use is not permitted by statutory regulation or exceeds the permitted use, you will need to obtain permission directly from the copyright holder.

